Hindawi
Journal of Nanomaterials
Volume 2022, Article ID 8020914, 10 pages
https://doi.org/10.1155/2022/8020914

Research Article

A Janus Mesh with Robust Interface and Controllable Wettability for Water Transport

Ziyi Guo,[1] Fengyun Guo,[1] Lei Gao,[1] Yan Wang,[1] and Yong Zhao[2]

[1]*Key Laboratory of Advanced Textile Materials and Fabrication Technology of Ministry of Education, School of Textile Science and Engineering (International Silk Institute), Zhejiang Sci-Tech University, Hangzhou 310018, China*
[2]*Key Laboratory of Bioinspired Intelligent Interface Science and Technology, Ministry of Education, School of Chemistry, Beihang University, Beijing 100191, China*

Correspondence should be addressed to Fengyun Guo; guofy@zstu.edu.cn

Received 16 November 2021; Revised 21 January 2022; Accepted 8 February 2022; Published 24 February 2022

Academic Editor: Mazeyar Parvinzadeh Gashti

The rational design of material structure is of great importance to the membrane material in water manipulation and management. Among them, by designing materials and structures on both sides of Janus membranes with porous structures, membranes with opposite wettability can be prepared to show directional liquid transport effects. However, the Janus membrane has the weakness of interfacial bonding due to the difference in the material and structure of the two layers. Here, we report a method to improve the interfacial bonding force of the two layers. Janus membrane is prepared using polyvinylidene fluoride hexafluoropropylene (PVDF-HFP) and cellulose acetate (CA) through the electrospinning method and then treated with sodium hydroxide (NaOH) solution. The as-prepared Janus membrane has a hydrophilic-hydrophobicity gradient and a strong bonding interface obtained by adjusting the chemical composition and microstructure. The NaOH solution plays a dominant role in forming hydrophilic-hydrophobicity gradient and enhancing the interface bonding between the bilayer membranes. The results show that this Janus membrane can achieve the purpose of oil-water separation and one-way water transmission by absorbing oil and regulating liquid surface tension. This strategy provides new ideas and technical supports for improving the Janus membrane interfacial bonding force and expands potential applications in the future.

1. Introduction

The advancement of industrialization has led to an increasingly outstanding problem of global water pollution, which has seriously affected human life and health [1]. Because of the severe situation of water pollution, the realization of sustainable development strategy requires the design and development of reliable water treatment technologies [2]. Traditional oily wastewater treatment methods include the air flotation method [3], flocculation method [4], solvent extraction method [5], biodegradation method [6], and adsorption method [7–9]. However, these methods have problems such as high cost, high energy consumption, and low efficiency. Therefore, the development of efficient and environmentally friendly oil-water separation technologies [10] and separation materials [11] can not only reduce environmental pollution but also recycle resources and create new value. In recent years, Janus membrane materials [12–15] have received extensive attention as an important research area in separation technology [16, 17]. Janus membrane refers to the asymmetry on both sides of the membrane, and this asymmetric anisotropy endows the Janus membrane with unique properties that distinguish it from homogeneous materials. In recent years, due to the asymmetry of the interface structure characteristics, Janus interface materials possessing of directional transmission characteristics have been used for liquid manipulation [18], high-efficiency oil-water separation [19, 20], and interface mass transfer [21, 22].

Electrospinning technology is simple and convenient and can effectively prepare fibrous materials [23]. The fiber obtained by electrospinning has the advantages of small diameter, large specific surface area, and high porosity [24, 25], which are very suitable for water transportation, liquid

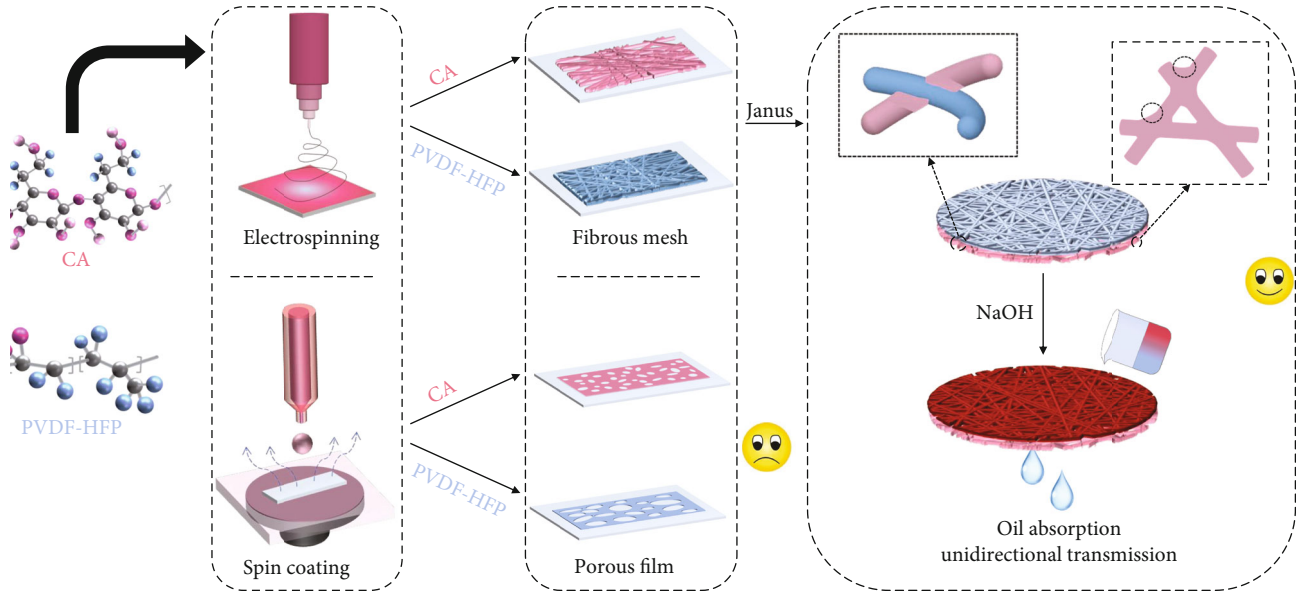

Figure 1: Schematic diagram of the experimental process. CA and PVDF-HFP are first prepared as porous membranes and fibrous membranes by spin-coating and electrospinning methods, respectively. The fibrous membranes obtained by electrospinning are then combined together to form PVDF-HFP/CA composite membrane and treated with NaOH to obtain PVDF-HFP/CA Janus membranes with strong interfacial adhesion, which made them good candidates for water transport.

separation, and so on. The morphology and structure of the fiber can be effectively controlled by changing the parameters to achieve the purpose of optimizing the fiber material [26–28]. Previous studies have proved that the directional transportation of liquids can be achieved by rationally designing the difference in the surface microstructure of the material [29, 30] or changing the chemical composition of the surface of the material [31]. For example, a group [32] prepared Janus membranes with different wettability on both sides, which can realize one-way oil delivery through electrospinning polyvinylidene fluoride (PVDF-HFP) and PVDP-HFP containing well-dispersed fluorinated decyl polyhedral oligomeric silsesquioxanes (FD-POSS) as well as fluorinated alkyl silane (FAS). Another group [33] used electrospinning to prepare hydrophobic PVDF fibrous membranes. The wettability of one side of the fibrous membrane was adjusted by electrospraying solutions containing different concentrations of hydrophilic or hydrophobic silica (SiO_2). Thus, a breathable Janus membrane is obtained. Our group also has done some researches and given some reviews on Janus fibrous membranes for liquid separation, water unidirectional transmission, and oil-water emulsion separation [15, 34, 35].

Although the previous researches have made great progress and promoted the development of this field, inevitably, there are still some problems. For example, the additional fluorosilane has side effects on the environment. In especial, the double-layer Janus membrane tends to be generally unstable with unfirmly bonded interface due to the bilayer structure of different materials. As a result, membrane delamination affects the separation effect after repeated applications. Based on the above background, herein, we report a type of Janus membranes (Figure 1). Using CA and PVDF-HFP as raw materials, the PVDF-HFP/CA double-layer fibrous membrane was prepared by electrospinning. By modifying the PVDF-HFP/CA fibrous membrane with NaOH treatment, the PVDF-HFP/CA Janus membrane is obtained with hydrophilic-hydrophobicity gradient, which can effectively absorb oily substances and permeate water unidirectionally to achieve the purpose of separation. Different from the previous reported Janus membrane obtained by electrospinning with the problem of weak interfacial bonding force, the alkali treatment can not only change the wettability of the CA membrane side but also improve the interfacial bonding by creating bonding points among fibers, making the PVDF-HFP/CA membrane a good candidate for robust Janus fibrous membrane. This method provides new ideas and technical support for the preparation of water management materials and has certain reference significance in the industrial and environmental fields.

2. Experiments and Methods

2.1. Experimental Materials and Instruments. CA (Mw = 30,000) and PVDF-HFP (Mw = 400,000) were purchased from Sigma-Aldrich in America. Deionized water, n-hexane, petroleum ether, methyl blue, Sudan III, and acetone were purchased from Zhejiang Hannuo Chemical Technology Co., Ltd. in China. N,N-Dimethylacetamide (DMAc) and NaOH were purchased from Hangzhou Gaojing Fine Chemical Co., Ltd. in China. The reagents mentioned above are of analytical pure grade. All the chemicals were used without any treatment.

The THZ-103B constant temperature shaker is from Shanghai Yiheng Technology Co., Ltd.; the electrospinning device is homemade; the AL204 electronic balance is from Mettler Toledo Instruments Co., Ltd.; the Vltra55 thermal field emission scanning electron microscope is from Carl

Zeiss SMT Pte Ltd.; the EZ4-type spin-coating apparatus is from Jiangsu Leibo Scientific Instrument Co., Ltd.; the Nicolet 5700 Fourier transmission infrared (FTIR) spectrometer is from USA Thermo Electron Corporation.

2.2. Spinning Solution Preparation. 2.4 g, 3.2 g, and 4 g of PVDF-HFP were weighed by an electronic balance, the mass ratio of acetone to DMAc was 7 : 3, and the total mass was 20 g spinning solution. The obtained solution concentrations were 12 wt%, 16 wt%, and 20 wt%, respectively. The solutions were stirred until the solids are completely dissolved. The CA spinning solution was made by dissolving CA in a mixture of DMAc and acetone (1 : 2 *v*/*v*) at concentrations of 15 wt%, 17.5 wt%, and 20 wt%, respectively. Three bottles of spinning solution were placed in a constant temperature shaker, dissolved at 37°C for 24 hours. The spinning solution was placed in a shaker and stirred until completely dissolved.

2.3. Electrospun Membrane Preparation. The 15 wt% concentration of CA spinning solution was poured into a 10 mL medical syringe and used with a 22-gauge needle. The receiving distance was controlled to 10 cm, and the spinning machine voltage was adjusted to 17.5 kV. The injector flow rate was set to 1 mL/h, and the drum speed was 300 r/min. After 2 hours, the membrane was obtained. Under the same spinning conditions, CA fibrous membranes with a concentration of 17.5 wt% and 20 wt% were sequentially spun.

The PVDF-HFP spinning solution was poured into a 10 mL medical syringe and used with a 21-gauge needle. The receiving distance was adjusted to 15 cm, the spinning voltage was set to 12 kV, the injection flow rate was 1 mL/h, and the drum speed was 300 r/min. After 70 minutes, the membrane was obtained. Under this condition, each PVDF-HFP fibrous membrane with a concentration of 12 wt%, 16 wt%, and 20 wt% was spun out.

After electrospinning 16 wt% PVDF-HFP under the above conditions for 30 min, a layer of 20 wt% CA was electrospun on the PVDF-HFP fibrous membrane, and the CA electrospinning time was 90 min. The prepared PVDF-HFP/CA double-layer fibrous membrane was placed in a NaOH solution with a concentration of 0.05 mol/L for 24 hours and then washed carefully with deionized water until neutral pH was achieved. The obtained membrane was then put into an oven at 40°C to fully dry, thereby obtaining PVDF-HFP/CA Janus membrane with different wettability on both sides.

2.4. Spin-Coating Membrane Preparation. The CA spinning solution and PVDF-HFP spinning solution were sucked 1 mL by the glue tip dropper, then dropped on the center of the glass slide, and placed in a spin coater to spin-coat into porous membranes. Spin-coating parameters were set to time 20 s and rotation speed 2000 rpm. After spin coating, the solvent evaporated to form a smooth porous membrane.

2.5. Structure and Performance Characterization. The thermal field emission scanning electron microscope (SEM) was used to observe the microscopic morphology of PVDF-HFP and CA membranes. The pore size distribution and fiber diameter distribution were counted by Nano Measurer and Origin software. Corresponding errors occur when using measurement software to measure. Choose fifty samples to get the average value and error bar.

The sample strip (3 cm × 2 cm) was stuck on the glass slide flatly with double-sided tape. The static contact angle measuring instrument was used to obtain the contact angle of water. The three-point circle method was used for contact angle statistics. Corresponding errors occur when using measurement software to measure. Choose five samples to obtain the average value and error bar.

2.6. Water Transport and Oil-Water Separation. N-Hexane was dyed blue by methyl blue, and water was dyed red by Sudan III. The mixture of n-hexane and water was dropped onto the PVDF-HFP surface of the Janus membrane, respectively.

3. Results and Discussions

The wettability of a material can be regulated by its microstructure and composition. In order to obtain the target material, we optimized the microstructure of the two materials firstly including porous membrane and fibrous membrane by spin coating and electrospinning (Figure 1). The SEM micrographs of the CA spin-coated membrane and PVDF-HFP spin-coated membrane are shown in Figure 2. Figures 2(a)–2(c) illustrate the morphology of CA spin-coated membrane with different concentrations and their corresponding enlarged views. It can be obviously observed from the figure that under the same spin-coating parameters, the spin-coated membrane of CA has lots of pores after solvent evaporation and drying. Similarly, PVDF-HFP spin-coated membrane (Figures 2(e)–2(g)) also shows a similar trend. The average pore diameters (Figure 2(d)) of 15 wt% CA, 17.5 wt% CA, and 20 wt% CA are 0.9 μm, 0.77 μm, and 0.03 μm, respectively. The average pore diameters (Figure 2(h)) of 12 wt% PVDF-HFP, 16 wt% PVDF-HFP, and 20 wt% PVDF-HFP are 2.91 μm, 0.75 μm, and 0.22 μm, respectively. The results demonstrate that under the same spin-coating parameters, the porous membrane obtained by spin coating with different concentrations is distributed with pores of different sizes. This is due to the volatilization of the acetone and DMAc during spin coating. The higher the concentration of the spinning solution is, the smaller the pores of the smooth membrane under the same magnification becomes. The spin-coating method is convenient and fast to prepare membranes, but spin-coated membranes with unreasonable pores and poor mechanical properties are not ideal candidates as separation materials. The fiber obtained by electrospinning has many applications in the field of filtration and separation because of their high porosity, large specific surface area, and uniform fiber diameter. Therefore, CA and PVDF-HFP fiber were prepared by electrospinning.

Figure 3 shows the SEM image and fiber diameter distribution diagram of CA fibrous membrane and PVDF-HFP fibrous membrane obtained by electrospinning with

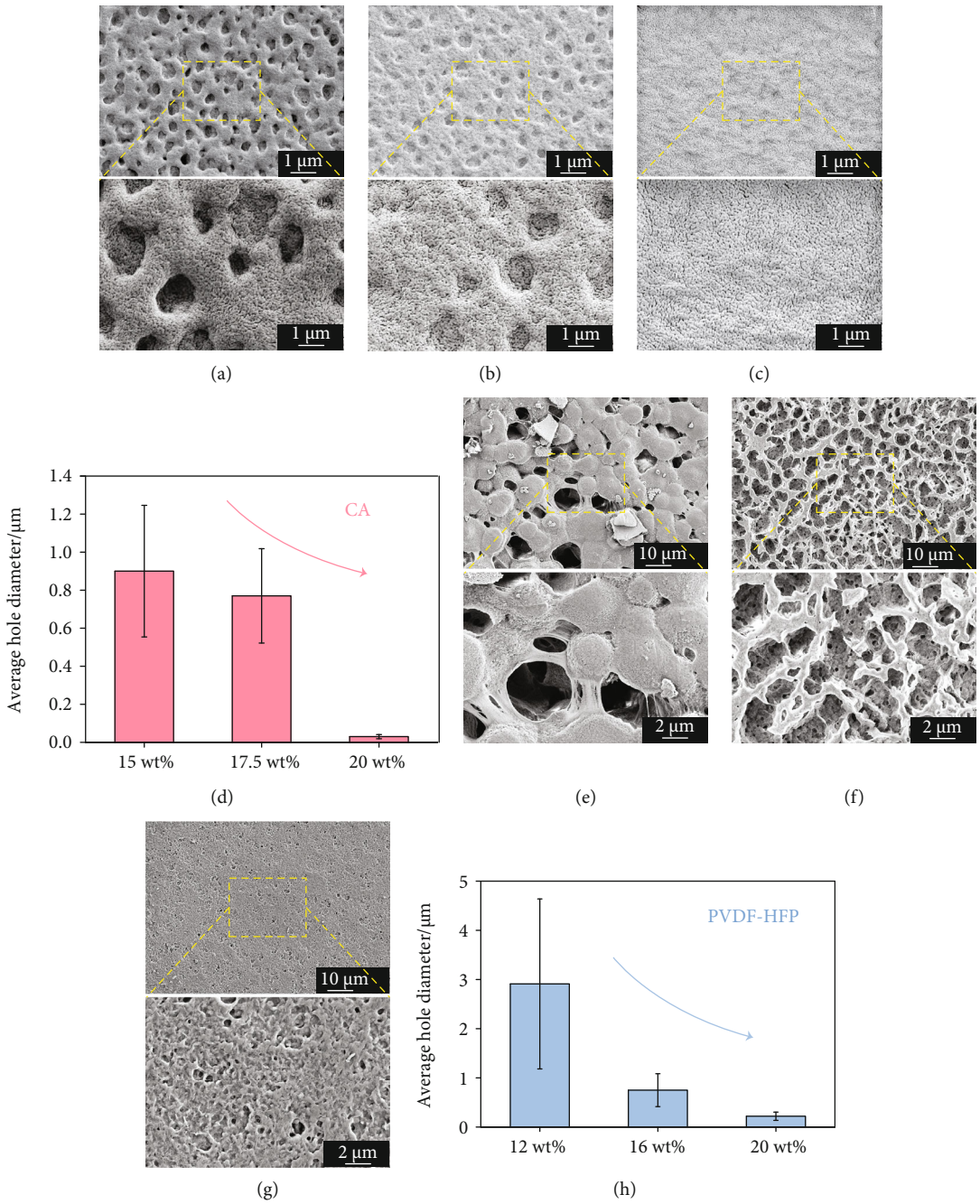

Figure 2: SEM images and pore size distribution of different concentrations of CA and PVDF-HFP spin-coated membranes. (a) SEM image of 15 wt% CA and its corresponding magnified image; (b) SEM image of 17.5 wt% CA and its corresponding magnified image; (c) SEM image of 20 wt% CA and its corresponding magnified image; (d) 15 wt%, 17.5 wt%, and 20 wt% CA pore size distribution; (e) SEM image of 12 wt% PVDF-HFP and its corresponding magnified image; (f) SEM image of 16 wt% PVDF-HFP and its corresponding magnified image; (g) SEM image of 20 wt% PVDF-HFP and its corresponding magnified image; (h) 12 wt%, 16 wt%, and 20 wt% PVDF-HFP pore size distribution. The yellow marks indicate the enlarged view of the morphology.

different concentrations. Figures 3(a)–3(c) reveal that the single CA fiber has irregular beads with a random orientation and varies in diameters. And, with the concentration increasing from 15 wt% to 20 wt%, the beads on the fiber gradually disappear, forming fibers without obvious defects. The average diameters of 15 wt% CA, 17.5 wt% CA, and 20 wt% CA fibers are 0.06 μm, 0.10 μm, and 0.18 μm, respectively (Figure 3(d)). The PVDF-HFP fiber (Figures 3(e)–3(g)) possesses a smooth and bead-free fibrous structure. The average diameters of 12 wt% PVDF-HFP, 16 wt% PVDF-HFP, and 20 wt% PVDF-HFP are 0.13 μm, 0.26 μm, and 0.64 μm, respectively (Figure 3(h)). The results show that the polymer solution concentration has a direct effect on the diameter of electrospun fibers. By changing the

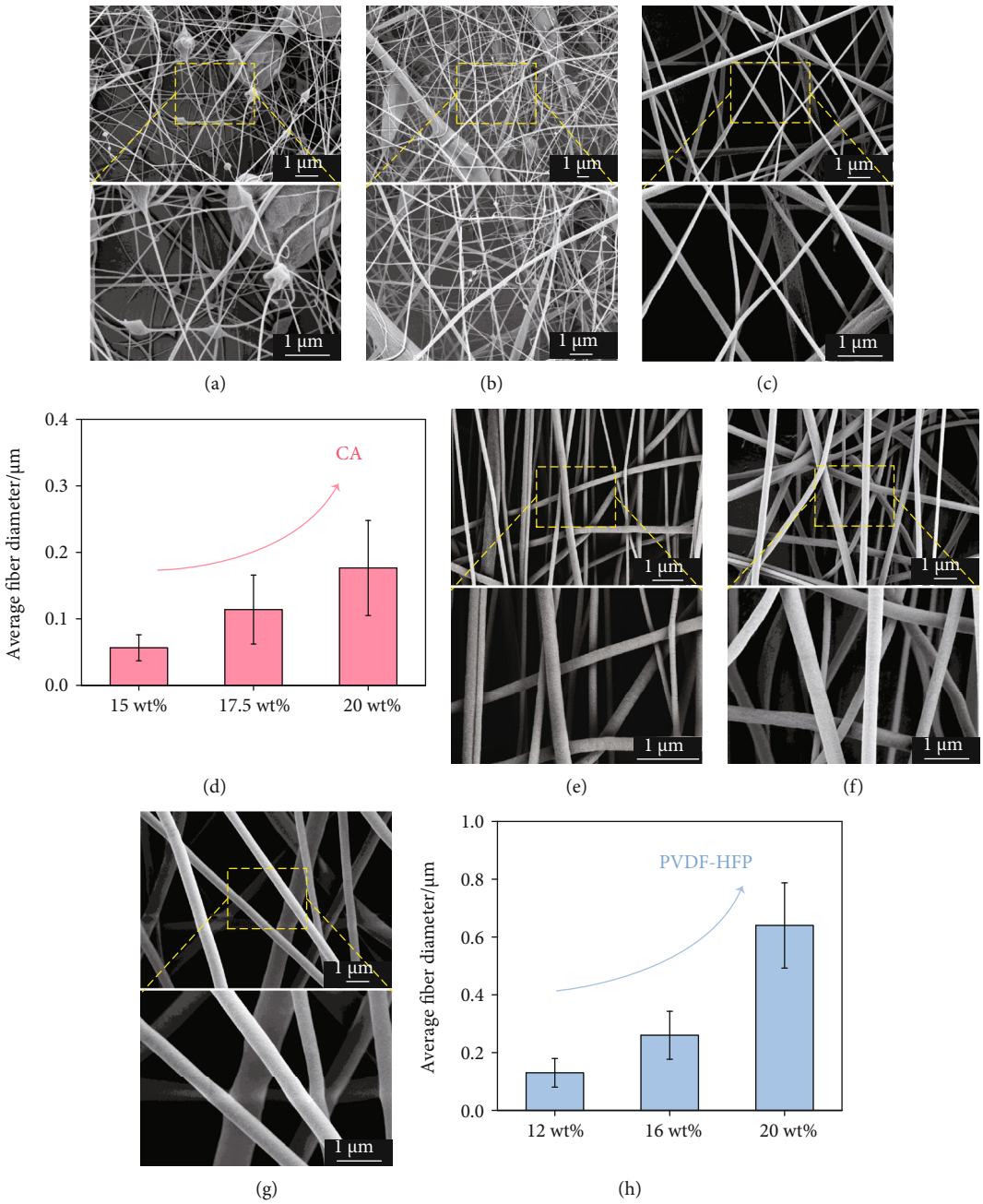

Figure 3: SEM images and diameter distribution diagrams of different concentrations of CA and PVDF-HFP electrospun membranes. (a) SEM images of 15 wt% CA fibers and their corresponding magnified images; (b) SEM images of 17.5 wt% CA fibers and their corresponding magnified images; (c) SEM images of 20 wt% CA fibers and their corresponding magnified images; (d) 15 wt%, 17.5 wt%, and 20 wt% diameter distribution of CA; (e) SEM images of 12 wt% PVDF-HFP fibers and their corresponding magnified images; (f) SEM images of 16 wt% PVDF-HFP fibers and their corresponding magnified images; (g) SEM images of 20 wt% PVDF-HFP fibers and their corresponding magnified images; (h) 12 wt%, 16 wt%, and 20 wt% diameter distribution of PVDF-HFP. The yellow marks indicate the enlarged view of the morphology.

polymer concentration during electrospinning, the fiber diameter will gradually increase with increasing solution concentration.

Next, the wettability of the membrane with porous structure and fibrous structure is investigated by water contact angle experiments. The hydrophilicity and hydrophobicity gradient characteristics are characterized in Figure 4. Figure 4(a) displays the wettability of different types of membranes. Figure 4(b) demonstrates the statistic contact angle values of different types of membranes. The CA and PVDF-HFP porous membranes exhibit hydrophilicity with a contact angle of 52.6° and hydrophobicity with a contact angle of 120.2°, while the corresponding fibrous membranes exhibit both hydrophobicities with a contact angle of 132.0° and 139.5°, respectively. Although CA and PVDF-HFP spin-coated porous membranes have a wetting gradient, the

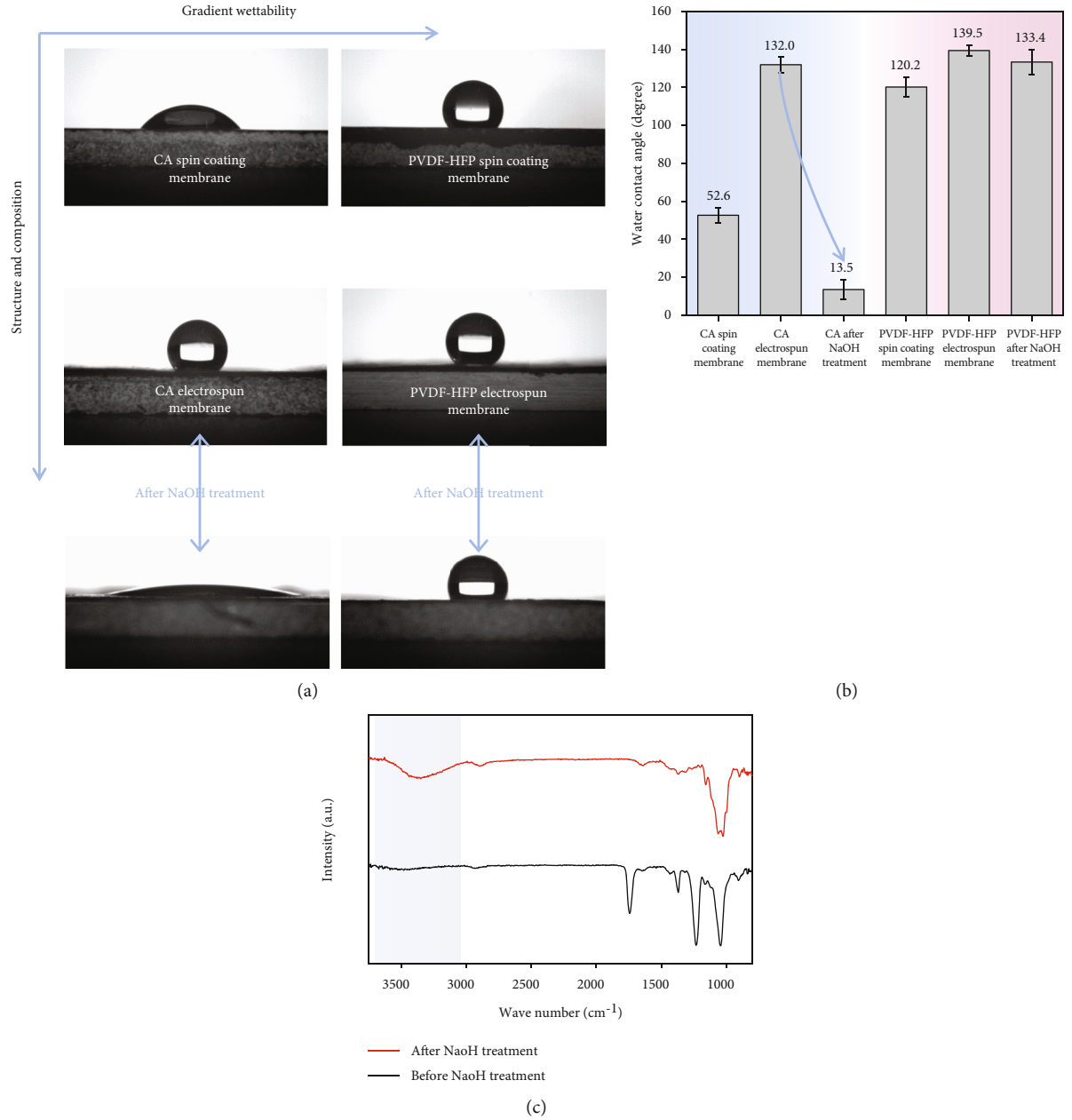

Figure 4: Hydrophilic and hydrophobic gradient properties of different materials and structures. (a) Contact angle of different types of membranes; (b) average value of contact angles of different types of membranes; (c) FTIR of composite membrane before and after NaOH treatment proving that CA is hydrolyzed.

mechanical properties of the spin-coated membranes are poor, and the two porous membranes cannot be well combined. Thus, the fibrous membranes are chosen as alternative. Both PVDF-HFP fibrous membrane and CA fibrous membrane exhibit hydrophobicity; however, Janus membranes generally require opposite wettability on both sides to achieve liquid permeation. Therefore, the fibrous membrane was hydrolyzed with NaOH to obtain wetting gradient. After being treated with 0.05 mol/L NaOH solution, the hydrophobic CA fibrous membrane (132.0°) became hydrophilic with a contact angle of 13.5°, achieving a large abrupt change in wetting gradient. In terms of PVDF-HFP, with an almost unchanged contact angle of 133.4°, it is still hydrophobic. To confirm the hydrolysis of CA, we carried out Fourier infrared (FTIR) spectrometer analysis. The results revealed that CA fibers can be well hydrolyzed after NaOH treatment. As shown in Figure 4(c), the characteristic adsorption peaks caused by the vibration of acetate groups C=O (1740), C=CH_3 (1370), and C-O-C (1225 cm^{-1}) were observed before NaOH treatment. After hydrolysis, the vibration peak of the acetic acid group almost disappeared, and the membrane after NaOH treatment showed a very obvious broadband between 3500 and 3100 cm^{-1}, indicating the existence of the hydrogen bond -OH group.

Therefore, in order to obtain a Janus membrane with integrated performance including strong bonding interface,

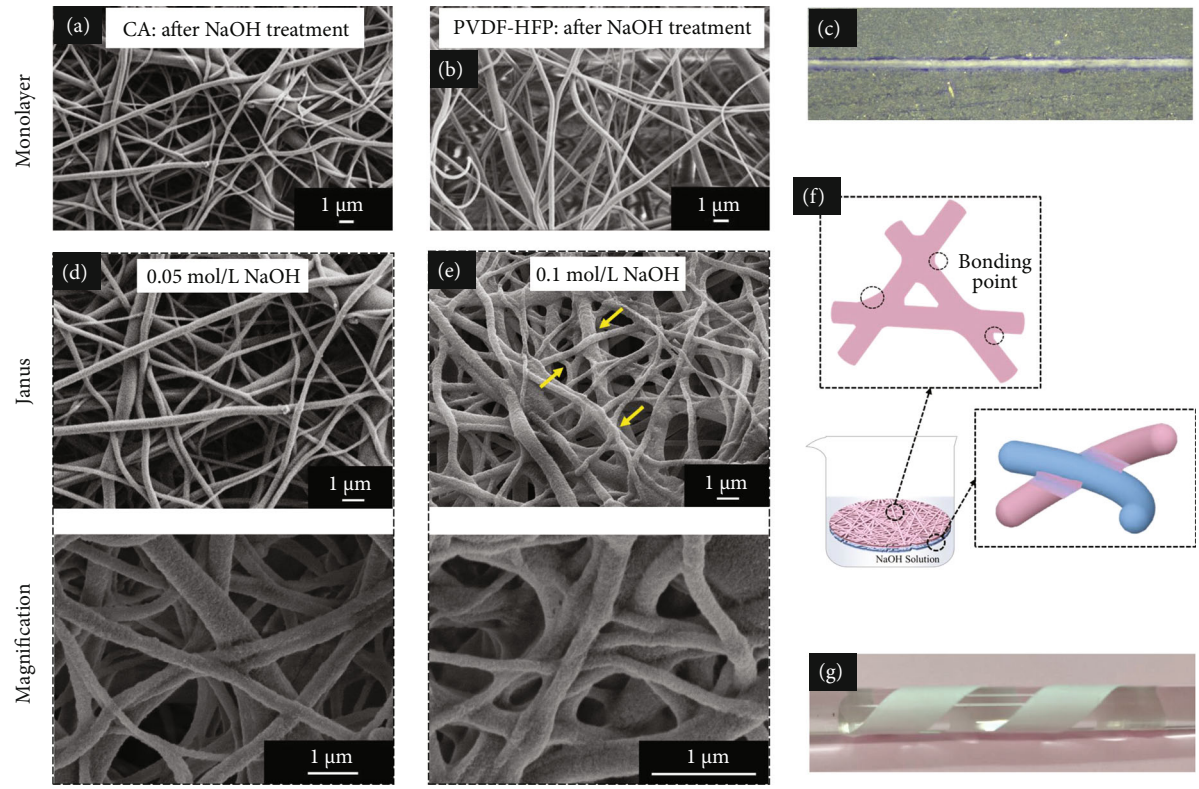

Figure 5: Bonding and welding morphology of PVDF-HFP/CA Janus membrane with robust surface and interface after NaOH treatment. (a) SEM image of CA fibers treated with 0.05 mol/L NaOH; (b) SEM image of PVDF-HFP fibers treated with 0.05 mol/L NaOH; (c) cross section of PVDF-HFP/CA Janus membrane under a microscope; (d) CA surface after 0.05 mol/L NaOH treatment and enlarged view; (e) CA surface after 0.1 mol/L NaOH treatment and enlarged view; (f) the schematic diagram of PVDF-HFP/CA composite membrane with bonding structure after NaOH treatment; (g) flexible and robust PVDF-HFP/CA Janus membrane can be wound on glass rods.

improved mechanical properties, and wetting gradient, the PVDF-HFP/CA double-layer fibrous membrane was treated with NaOH. The surface-interface structure and the morphology evolution under different NaOH concentrations were investigated (Figure 5). We first prepared PVDF-HFP/CA double-layer membrane through "layer-by-layer" electrospinning. In order to construct the opposite wettability between PVDF-HFP/CA membrane, the PVDF-HFP/CA double-layer membrane was soaked in a 0.05 mol/L NaOH solution in 24 h to make the CA fibrous membrane hydrophilic. The performance of the PVDF-HFP/CA Janus membrane formed after NaOH treatment is given in Figure 5. Figures 5(a) and 5(b) are SEM images of both sides of the PVDF-HFP/CA Janus membrane after being treated with 0.05 mol/L NaOH solution. After being treated, the individual fibers on the surface of the CA fibrous membrane are bonded to each other, and connecting points are formed at the joints, making the fibers stick together (Figure 5(a)). The microstructure of PVDF-HFP fibrous membrane treated with NaOH solution hardly changes, and there are no connection points between the fibers (Figure 5(b)). The cross-sectional view of the PVDF-HFP/CA Janus membrane (Figure 5(c)) obtained after NaOH treatment reveals that the double-layer membrane is not separated, which can make the membrane performance more stable.

The "layer-by-layer" approach of electrospun Janus membranes should consider strengthening the bonding performance between the interfaces to obtain membranes with excellent stability. Therefore, we examined the effect of NaOH concentration on bonding degree. SEM images show that different concentrations of NaOH treatment will produce different degrees of adhesion on the CA surface and interface (Figures 5(d)–5(f)). After 0.1 mol/L NaOH treatment (Figure 5(e)), the degree of adhesion between CA fibers is significantly higher than that of 0.05 mol/L NaOH treatment (Figure 5(d)). However, the high degree of adhesion is also accompanied by a decrease in the flux between the fibers, which affect the efficiency of liquid transportation. Overall, the NaOH treatment can not only endow the PVDF-HFP/CA composite membrane asymmetric wetting properties but also enhance the bonding force between the two fibrous membranes. Figure 5(f) demonstrates the schematic diagram of PVDF-HFP/CA Janus membrane with bonding after NaOH treatment. After PVDF-HFP/CA composite membrane is immersed in the NaOH solution, the side of CA fibrous membrane will be hydrolyzed to produce connection points at the fiber surface connection. The CA fibrous membrane will also adhere to the PVDF-HFP fibrous membrane under the action of the NaOH solution, thereby improving the bonding between the two layers of fibrous membranes. The as-prepared PVDF-HFP/CA Janus membranes show excellent mechanical properties (Figure 5(g)) due to bonding structure. The existence of bonding points between the fibers increases the mechanical properties of

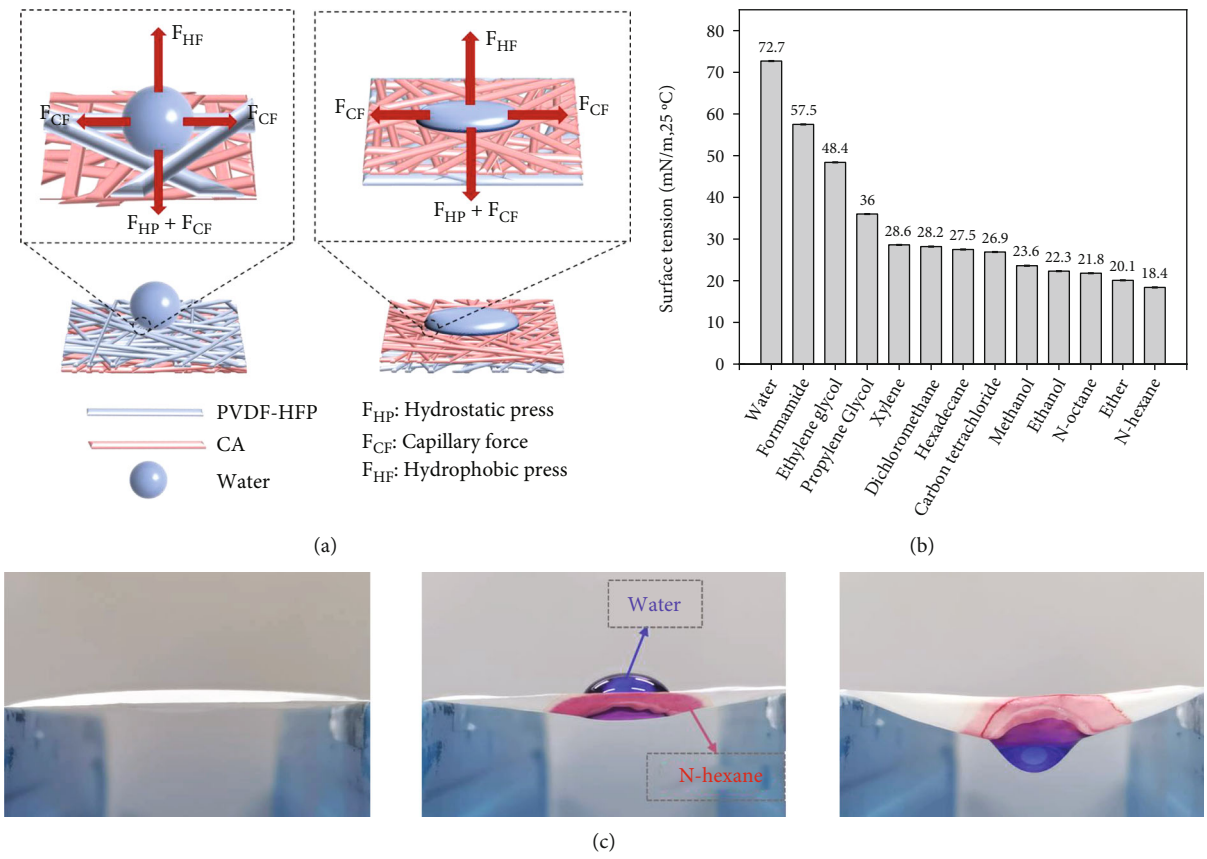

FIGURE 6: The mechanism diagram and demonstration of Janus membrane for oil-water separation. (a) A possible mechanism diagram of PVDF-HFP/CA Janus membrane for liquid transport; (b) statistics of surface tension of different liquids; (c) PVDF-HFP/CA Janus membrane oil-water separation demonstration, which can separate the mixed liquid of water and n-hexane.

the Janus membrane to a certain extent. Compared with traditional filter membranes such as ceramic sintered membranes and metal sintered membranes, the excellent bonding structure and mechanical properties make fibrous membranes a better candidate.

Figure 6 is the mechanism diagram and demonstration of Janus membrane for oil-water separation. A design rule and mechanism for the water transportation and oil-water separation of PVDF-HFP/CA Janus membranes is illustrated in Figure 6(a). Liquid transport in porous fibers is a complex phenomenon, and the ability to achieve liquid transport is the result of the combined effects of multiple factors, such as the chemical properties of the material surface, surface roughness, and porosity. The unidirectional permeation of liquid in porous Janus materials is essentially caused by the critical breakthrough pressure difference of the liquid from the hydrophobic layer to the hydrophilic layer, and the difference in critical breakthrough pressure on both sides of the Janus interface promotes the unidirectional transport of water [36, 37]. The surface chemistry of the material works when the droplet contacts the surface of the material. Once the surface chemistry of the material can provide space for water transport, the porosity of the surface activates the capillary force (F_{CF}) of the fiber material at this time, allowing water droplets to quickly pass through the fiber material. Water transportation on Janus membranes can be divided into two cases. One is the transportation from the hydrophobic layer to the hydrophilic layer, and the other is the transportation from the hydrophilic layer to the hydrophobic layer. When the water droplets are on the hydrophobic layer, the water droplets remain spherical. At this time, a downward hydrostatic pressure (F_{HP}) is generated at the liquid-air interface and the hydrophobic force (F_{HF}) that prevents water from passing through the PVDF-HFP. When the F_{HP} is large enough to overcome the water transportation barrier force (F_{HF}) on the hydrophobic side, the water will be pushed towards the hydrophilic layer. In addition, the wetting gradient between the two fibrous membranes and the pores between the electrospun fibers will further excite the water droplets to penetrate the hydrophobic layer. Once the water droplets reach the surface of the hydrophilic layer, the hydrophilicity and capillary force (F_{CF}) on the surface of the hydrophilic layer can rapidly spread the water droplets in all directions within the hydrophilic layer. Finally, the water droplets will collect on the surface of the hydrophilic layer. On the contrary, when the water droplets are on the hydrophilic layer, the hydrophilic nature of the hydrophilic layer and the capillary force (F_{CF}) will make the water droplets diffuse rapidly into the membrane on the hydrophilic side. At this time, the pressure F_{HP}

required for penetration is limited, so that water droplets cannot pass through the hydrophilic layer to the hydrophobic layer. All in all, the transmembrane pressure on the hydrophilic side is much greater than that on the hydrophobic side. Due to the difference in surface tension between liquids, when different liquids are mixed and separated, the fibrous membrane will allow the wettable liquid below the membrane surface tension to pass through, while blocking another nonwettable liquid with high surface tension. In other words, when the surface energy of the fibrous membrane is just between the surface energy of the two mixed liquids, it can be used to separate the mixed liquid. Thus, we measured the surface tension of different liquids as presented in Figure 6(b). The surface tension of water is 72.7 mN/m, while the surface tension of n-hexane is 18.4 mN/m. The difference in the surface tension will affect the liquid transmission and separation behavior. Based on the above concept, we demonstrated the oil-water separation process of Janus membrane (Figure 6(c)) using n-hexane and water as an example. First, a mixture of n-hexane liquid dyed red and water dyed blue is dropped onto the PVDF-HFP surface of the Janus membrane. The results clearly show that the n-hexane diffuses on the fibrous membrane and is adsorbed by the Janus membrane, while the water droplets on the hydrophobic PVDF-HFP side can penetrate the PVDF-HFP side to the hydrophilic CA surface and finally fall. According to the theory of surface tension affecting liquid transmission, we also did the separation experiment of the mixture with other oil and water in the same way and got similar experimental results. The demonstration experiment of PVDF-HFP/CA Janus membrane visually confirmed the ability of the prepared membrane to separate oil-water mixture. To sum up, the NaOH treatment imparts a wetting gradient and bonding structure to the fibrous membrane so that the membrane can realize water transmission and oil-water separation without delamination.

In this work, aiming at solving the problem of unstable interfacial bonding of bilayer Janus membranes formed by simple superposition, we used alkali treatment to improve the interfacial bonding force between layers. This will help to improve the structural stability of electrospun Janus membranes, thereby increasing the practical application of Janus membranes in liquid unidirectional permeation, oil-water separation, and seawater desalination.

4. Conclusions

In summary, we propose a method to prepare robust interfacial bonding between Janus membranes. PVDF-HFP/CA Janus membranes with strong adhesion and controlled wettability were prepared by using electrospinning and NaOH soaking. NaOH treatment can not only build a hydrophilic-hydrophobic gradient between the bilayer membranes but also create a bonding structure between fibers to enhance the interfacial bonding force. By adjusting the surface tension of the liquid, the prepared Janus membrane can maintain a stable fiber interface during the process of unidirectional oil absorption and water delivery. This strategy provides new ideas and technical support for the preparation of composite fibrous membranes having a firm interface, expanding the application range of Janus membranes.

Data Availability

The data used to support the findings of this study are included within the article.

Conflicts of Interest

The authors declared that they have no conflicts of interest to this work.

Acknowledgments

This work is supported by the National Natural Science Foundation of China, Grants 51803183.

References

[1] X. Xu, S. Ozden, N. Bizmark, C. B. Arnold, S. S. Datta, and R. D. Priestley, "A bioinspired elastic hydrogel for solar-driven water purification," *Advanced Materials*, vol. 33, no. 18, 2021.

[2] N. L. Le and S. P. Nunes, "Materials and membrane technologies for water and energy sustainability," *Materials and Technologies*, vol. 7, pp. 1–28, 2016.

[3] J. Saththasivam, K. Loganathan, and S. Sarp, "An overview of oil-water separation using gas flotation systems," *Chemosphere*, vol. 144, pp. 671–680, 2016.

[4] C. Rattanapan, A. Sawain, T. Suksaroj, and C. Suksaroj, "Enhanced efficiency of dissolved air flotation for biodiesel wastewater treatment by acidification and coagulation processes," *Desalination*, vol. 280, no. 1-3, pp. 370–377, 2011.

[5] C. Yang, Y. Qian, L. Zhang, and J. Feng, "Solvent extraction process development and on-site trial-plant for phenol removal from industrial coal-gasification wastewater," *Chemical Engineering Journal*, vol. 117, no. 2, pp. 179–185, 2006.

[6] K. I. Suehara, Y. Kawamoto, E. Fujii, J. Kohda, Y. Nakano, and T. Yano, "Biological treatment of wastewater discharged from biodiesel fuel production plant with alkali-catalyzed transesterification," *Journal of Bioscience and Bioengineering*, vol. 100, no. 4, pp. 437–442, 2005.

[7] W. Pitakpoolsil and M. Hunsom, "Adsorption of pollutants from biodiesel wastewater using chitosan flakes," *Journal of the Taiwan Institute of Chemical Engineers*, vol. 44, no. 6, pp. 963–971, 2013.

[8] S. Sankaranarayanan, D. S. Lakshmi, S. Vivekanandhan, and C. Ngamcharussrivichai, "Biocarbons as emerging and sustainable hydrophobic/oleophilic sorbent materials for oil/water separation," *Sustainable Materials and Technologies*, vol. 28, 2021.

[9] P. Kumari, M. Alam, and W. A. Siddiqi, "Usage of nanoparticles as adsorbents for waste water treatment: an emerging trend," *Sustainable Materials and Technologies*, vol. 22, 2019.

[10] Y. Lin, M. Sameh, L. Zhang, Q. Shen, and H. Matsuyama, "Development of Janus membrane with controllable asymmetric wettability for highly-efficient oil/water emulsions separation," *Journal of Membrane Science*, vol. 606, 2020.

[11] Y. Wang, J. Di, L. Wang et al., "Infused-liquid-switchable porous nanofibrous membranes for multiphase liquid separation," *Nature Communications*, vol. 8, no. 1, p. 575, 2017.

[12] H. N. Li, J. Yang, and Z. K. Xu, "Asymmetric surface engineering for Janus membranes," *Advanced Materials Interfaces*, vol. 7, no. 7, 2020.

[13] H. C. Yang, J. Hou, V. Chen, and Z. K. Xu, "Janus membranes: exploring duality for advanced separation," *Angewandte Chemie International Edition*, vol. 55, no. 43, pp. 13398–13407, 2016.

[14] S. W. Ng, N. Noor, and Z. J. Zheng, "Graphene-based two-dimensional Janus materials," *NPG Asia Materials*, vol. 10, no. 4, pp. 217–237, 2018.

[15] L. L. Hou, N. Wang, X. K. Man, Z. M. Cui, and Y. Zhao, "Interpenetrating Janus membrane for high rectification ratio liquid unidirectional penetration," *ACS Nano*, vol. 13, no. 4, pp. 4124–4132, 2019.

[16] M. Padaki and R. S. Murali, "Membrane technology enhancement in oil–water separation. A review," *Desalination*, vol. 357, pp. 197–207, 2015.

[17] H. Wang, H. Zhou, H. Niu, J. Zhang, Y. Du, and T. Lin, "Dual-layer superamphiphobic/superhydrophobic-oleophilic nanofibrous membranes with unidirectional oil-transport ability and strengthened oil–water separation performance," *Advanced Materials Interfaces*, vol. 2, no. 4, 2015.

[18] T. Li, F. Liu, S. Zhang, H. Lin, J. Wang, and C. Tang, "Janus polyvinylidene fluoride membrane with extremely opposite wetting surfaces via one single-step unidirectional segregation strategy," *ACS Applied Materials & Interfaces*, vol. 10, no. 29, pp. 24947–24954, 2018.

[19] Z. J. Wang, Y. Wang, and P. G. Liu, "Rapid and efficient separation of oil from oil-in-water emulsions using a Janus cotton fabric," *Angewandte Chemie*, vol. 128, no. 4, pp. 1313–1316, 2016.

[20] Z. Wang, X. Liu, J. Guo, T. A. Sherazi, and S. Li, "A liquid-based Janus porous membrane for convenient liquid–liquid extraction and immiscible oil/water separation," *Chemical Communications*, vol. 55, no. 96, pp. 14486–14489, 2019.

[21] Y. J. Li, H. Zhang, T. H. Xu et al., "Under-water superaerophobic pine-shaped Pt nanoarray electrode for ultrahigh- performance hydrogen evolution," *Advanced Functional Materials*, vol. 25, no. 11, pp. 1737–1744, 2015.

[22] J. Hou, J. Chao, G. Dong, B. Xiao, Y. Yun, and V. Chen, "Biocatalytic Janus membranes for CO_2 removal utilizing carbonic anhydrase," *Journal of Materials Chemistry A*, vol. 3, no. 33, pp. 17032–17041, 2015.

[23] J. J. Xue, T. Wu, Y. Q. Dai, and Y. N. Xia, "Electrospinning and electrospun nanofibers: methods, materials, and applications," *Chemical Reviews*, vol. 119, no. 8, pp. 5298–5415, 2019.

[24] D. Li and Y. Xia, "Electrospinning of nanofibers: reinventing the wheel?," *Advanced Materials*, vol. 16, no. 14, pp. 1151–1170, 2004.

[25] N. Thakur, A. Baji, and A. S. Ranganath, "Thermoresponsive electrospun fibers for water harvesting applications," *Applied Surface Science*, vol. 433, pp. 1018–1024, 2018.

[26] B. Cheng, Z. J. Li, Q. X. Li, J. G. Ju, W. M. Kang, and M. Naebe, "Development of smart poly(vinylidene fluoride)-graft-poly(-acrylic acid) tree- like nanofiber membrane for pH-responsive oil/water separation," *Journal of Membrane Science*, vol. 534, pp. 1–8, 2017.

[27] A. S. Ranganath and A. Baji, "Electrospun Janus membrane for efficient and switchable oil–water separation," *Macromolecular Materials and Engineering*, vol. 303, no. 11, p. 1800272, 2018.

[28] T. Zhang, C. Xiao, J. Zhao, X. Liu, D. Ji, and H. Zhang, "One-step facile fabrication of PVDF/graphene composite nanofibrous membrane with enhanced oil affinity for highly efficient gravity-driven emulsified oil/water separation and selective oil absorption," *Separation and Purification Technology*, vol. 254, 2020.

[29] Y. M. Hou, M. Yu, X. M. Chen, Z. K. Wang, and S. H. Yao, "Recurrent filmwise and dropwise condensation on a beetle mimetic surface," *ACS Nano*, vol. 9, no. 1, pp. 71–81, 2015.

[30] Z. Yu, F. Yun, Y. Wang et al., "Desert beetle-inspired superwettable patterned surfaces for water harvesting," *Small*, vol. 13, no. 36, 2017.

[31] M. Doukkali, E. Gauthier, R. B. Patel, V. Stepanov, and H. Hadim, "Modifying the wettability of nitramine explosives using anionic, cationic and nonionic surfactants," *Propellants, Explosives, Pyrotechnics*, vol. 42, no. 10, pp. 1185–1190, 2017.

[32] C. Yao, M. Luo, H. Wang, B. Xu, and Z. Cai, "Asymmetric wetting Janus fabrics with double-woven structure for oil/water separation," *Journal of Materials Science*, vol. 54, no. 7, pp. 5942–5951, 2019.

[33] Z. Zhigao, L. Zhiquan, Z. Lingling et al., "Breathable and asymmetrically superwettable Janus membrane with robust oil-fouling resistance for durable membrane distillation," *Journal of Membrane Science*, vol. 563, pp. 602–609, 2018.

[34] G. C. Yue, Y. Q. Wang, D. M. Li et al., "Bioinspired surface with special wettability for liquid transportation and separation," *Sustainable Materials and Technologies*, vol. 25, 2020.

[35] L. L. Hou, L. Wang, N. Wang et al., "Separation of organic liquid mixture by flexible nanofibrous membranes with precisely tunable wettability," *NPG Asia Materials*, vol. 8, no. 12, 2016.

[36] C. Chen, D. Weng, A. Mahmood, S. Chen, and J. Wang, "Separation mechanism and construction of surfaces with special wettability for oil/water separation," *ACS Applied Materials & Interfaces*, vol. 11, no. 11, pp. 11006–11027, 2019.

[37] C. K. Söz, S. Trosien, and M. Biesalski, "Janus interface materials: a critical review and comparative study," *ACS Materials Letters*, vol. 2, no. 4, pp. 336–357, 2020.